HGG Advances

REPORT

Somatic activating *BRAF* variants cause isolated lymphatic malformations

Kaitlyn Zenner,[1,2] Dana M. Jensen,[3] Victoria Dmyterko,[3] Giridhar M. Shivaram,[4] Candace T. Myers,[5] Cate R. Paschal,[5] Erin R. Rudzinski,[5] Minh-Hang M. Pham,[6] V. Chi Cheng,[6] Scott C. Manning,[1] Randall A. Bly,[1,2] Sheila Ganti,[1,2,7] Jonathan A. Perkins,[1,2] and James T. Bennett[2,3,8,*]

Summary

Somatic activating variants in *PIK3CA*, the gene that encodes the p110α catalytic subunit of phosphatidylinositol 3-kinase (PI3K), have been previously detected in ~80% of lymphatic malformations (LMs).[1,2] We report the presence of somatic activating variants in *BRAF* in individuals with LMs that do not possess pathogenic *PIK3CA* variants. The BRAF substitution p.Val600Glu (c.1799T>A), one of the most common driver mutations in cancer, was detected in multiple individuals with LMs. Histology revealed abnormal lymphatic channels with immunopositivity for $BRAF^{V600E}$ in endothelial cells that was otherwise indistinguishable from *PIK3CA*-positive LM. The finding that *BRAF* variants contribute to low-flow LMs increases the complexity of prior models associating low-flow vascular malformations (LM and venous malformations) with mutations in the PI3K-AKT-MTOR and high-flow vascular malformations (arteriovenous malformations) with mutations in the RAS-mitogen-activated protein kinase (MAPK) pathway.[3] In addition, this work highlights the importance of genetic diagnosis prior to initiating medical therapy as more studies examine therapeutics for individuals with vascular malformations.

Disorganized morphogenesis of arteries, veins, capillaries, and lymphatic vessels results in vascular malformations, a relatively common congenital malformation associated with significant morbidity.[4] Vascular malformations are classified into high-flow lesions, which include arteriovenous malformations (AVMs), and low-flow lesions, which include venous malformations (VeMs) and lymphatic malformations (LMs). Individuals with vascular malformations typically have no family history, because most are caused by post-zygotic (mosaic) activating mutations in oncogenes within the phosphatidylinositol 3-kinase (PI3K)-AKT and RAS-mitogen-activated protein kinase (MAPK) pathways.[1–3] Treatments for vascular malformations are primarily invasive and include sclerotherapy, embolization, and open surgical resection,[4] but the identification of specific activating mutations in well-known oncogenic signaling pathways has led to trials examining the efficacy of targeted medical therapies.[5–11]

Previous work has shown that approximately 80% of isolated LMs have somatic pathogenic variants in *PIK3CA*,[1,2,12] the gene that encodes for the catalytic subunit of PI3K, a component of the PI3K-AKT pathway.[13] Although mutations in other genes (including *NRAS*, *KRAS*, *CBL*, *ARAF*, and *EPHB4*) have been identified in complex lymphatic anomalies, such as diffuse lymphangiomatosis and Gorham-Stout disease,[14] *PIK3CA* is the only gene associated with isolated LMs to date. The vast majority (>90%) of LM-associated pathogenic variants occur at one of three locations,[2] referred to as "hotspots": c.1624G>A (p.Glu542Lys), c.1633G>A (p.Glu545Lys), and c.3140A>G (p.His1047Arg), all of which result in PI3K hyperactivation.[15,16] The fraction of DNA molecules that possess the pathogenic *PIK3CA* variant (referred to as the variant allele fraction [VAF]) within LM tissue is typically very low (<10%),[2] and it has been hypothesized that a fraction of LMs without a detected *PIK3CA* variant in fact do carry a *PIK3CA* variant that was "missed" due to low-level mosaicism. It is also possible that additional genes play a role. Here, we report the identification of somatic *BRAF* mutations in LMs without a detected *PIK3CA* variant.

LM tissue from 106 individuals was screened for the three *PIK3CA* (GenBank: NM_006218.4) hotspots (p.Glu542Lys, p.Glu545Lys, and p.His1047Arg) as well as the less common but amplicon-overlapping p.His1047Leu substitution using droplet digital polymerase chain reaction (ddPCR) assays and molecular inversion probes, as previously reported (Supplemental methods).[2] Following this screening, 22 individuals remained without a detected *PIK3CA* variant. Fifteen of these individuals had sufficient DNA (14 lesion-derived and 1 cyst fluid) for further testing, which was sent for high-depth targeted sequencing using a 44-gene panel, referred to as VANseq (vascular anomaly

[1]Seattle Children's Hospital, Division of Pediatric Otolaryngology, Department of Otolaryngology/Head and Neck Surgery, University of Washington, Seattle, WA 98195, USA; [2]Vascular Anomalies Program, Seattle Children's Hospital, Seattle, WA 98105, USA; [3]Center for Developmental Biology and Regenerative Medicine, Seattle Children's Research Institute, Seattle, WA 98101, USA; [4]Department of Radiology, Division of Interventional Radiology, University of Washington School of Medicine, Seattle, WA, USA; [5]Department of Laboratories, Seattle Children's Hospital, Seattle, WA 98105, USA; [6]Center for Integrative Brain Research, Seattle Children's Research Institute, Seattle, WA 98101, USA; [7]Center for Clinical and Translational Research, Seattle Children's Research Institute, Seattle, WA 98101, USA; [8]Seattle Children's Hospital, Division of Genetic Medicine, Department of Pediatrics, University of Washington, Seattle, WA 98195, USA

*Correspondence: jtbenn@uw.edu

https://doi.org/10.1016/j.xhgg.2022.100101.

Table 1. Somatic variants in LM detected by VANseq and confirmed by ddPCR

					VANseq reads			ddPCR droplets		
Subject	**Age[a]**	**Sex**	**Variant**	**Sample**	**VAF (%)**	**Var**	**WT**	**VAF[b] (%)**	**Var**	**WT**
LR18-536	2 years	F	*PIK3CA* p.Asn345Lys	lesion A	1.3	21	1,669	1.1	144	13,401
				lesion B	–	–	–	0.2	23	10,709
				lesion C	–	–	–	NEG	5	12,251
				lesion D	–	–	–	0.2	22	12,569
				lesion E	–	–	–	1.4	151	10,827
				lesion F	–	–	–	0.5	88	23,161
				lesion G	–	–	–	0.9	74	9,877
				skin	–	–	–	0.3	30	9,480
				salivary gland	–	–	–	NEG	0	31,662
LR16-278	2 years	F	*PIK3CA* p.Glu545Lys	lesion	0.7	12	1,709	0.5	48	12,295
LR16-264	3 years	F	*PIK3CA* p.Glu545Lys	lesion	10.6	7	59[c]	4.8	437	9,551
LR17-322	1 year	M	*BRAF* p.Val600Glu	lesion	2.1	34	1,618	1.7	165	10,555
				skin	–	–	–	NEG	0	10,374
LR19-346	5 months	F	*BRAF* p.Val600Glu	lesion, deep	0.6	7	1,143	1.2	69	5,872
				lesion, inferior	–	–	–	0.9	56	6,389
				lesion, superior	–	–	–	NEG	2	9,584
				lesion, no location	–	–	–	3.6	91	2,479
				skin	–	–	–	NEG	0	4,304
				fat	–	–	–	NEG	1	5,340
				muscle	–	–	–	NEG	0	6,129
LR19-443	1 month	M	*BRAF* p.Val600Glu	cyst fluid, A[d]	–	–	–	0.2	29	13,055
				cyst fluid, B[d]	0.3	4	1,458	0.1	10	9,661
				cyst fluid, C[d]	–	–	–	0.3	31	13,292
				cyst fluid pellet	–	–	–	NEG	15	30,798

ddPCR, droplet digital polymerase chain reaction; NEG, no variant detected; VAF, variant allele fraction; Var, variant; WT, wild type.
[a]Age at time of tissue or cyst fluid attainment.
[b]ddPCR VAF calculated using droplet concentrations and only reported for samples in which sample variant concentration was statistically different from WT control variant concentration based on 95% total error confidence intervals.
[c]Lower than typical coverage.
[d]Cell-free DNA was assayed from cyst fluid samples.

sequencing) (see Supplemental methods and Table S1) throughout the rest of this paper.

VANseq identified variants in 6/15 individuals (Table 1). One individual (LR18-536) had a non-hotspot *PIK3CA* variant, c.1035T>A (p.Asn345Lys) that could not have been detected by hotspot allele-specific ddPCR screening. This variant is absent from the Genome Aggregation Database (gnomAD), is predicted to be damaging by several *in silico* tools, and has been previously reported in numerous individuals with cancer as well as one individual with congenital lipomatous overgrowth, vascular malformations, epidermal nevis, spinal/skeletal anomalies/scoliosis (CLOVES) syndrome.[1,17,18] Functional studies have demonstrated that this substitution results in PI3K pathway hyperactivity.[15,16] Although not previously reported in association with isolated LMs, we interpreted this variant as being pathogenic[19] and confirmed the presence of the variant in additional samples from that individual using ddPCR. There was variation in VAF from undetectable to 1.4% within lesion samples (Table 1), as we have previously described.[2]

VANseq detected a hotspot *PIK3CA* variant (p.Glu545Lys) in two individuals (LR16-278 and LR16-264) who had previously been screened for this allele by ddPCR.[2] We re-examined prior data from both cases. LR16-278's prior ddPCR had six variants and 1,055 reference droplets but did not meet our positive criteria, as the 95% confidence interval overlapped with wild-type samples (Supplemental methods). The initial ddPCR run for LR16-264 had one variant and 5,305 reference droplets, but subsequent testing from the original stock DNA dilution was unambiguously positive by VANseq and ddPCR (VAFs of 10.6% and 4.8%, respectively). Although provenance testing was not

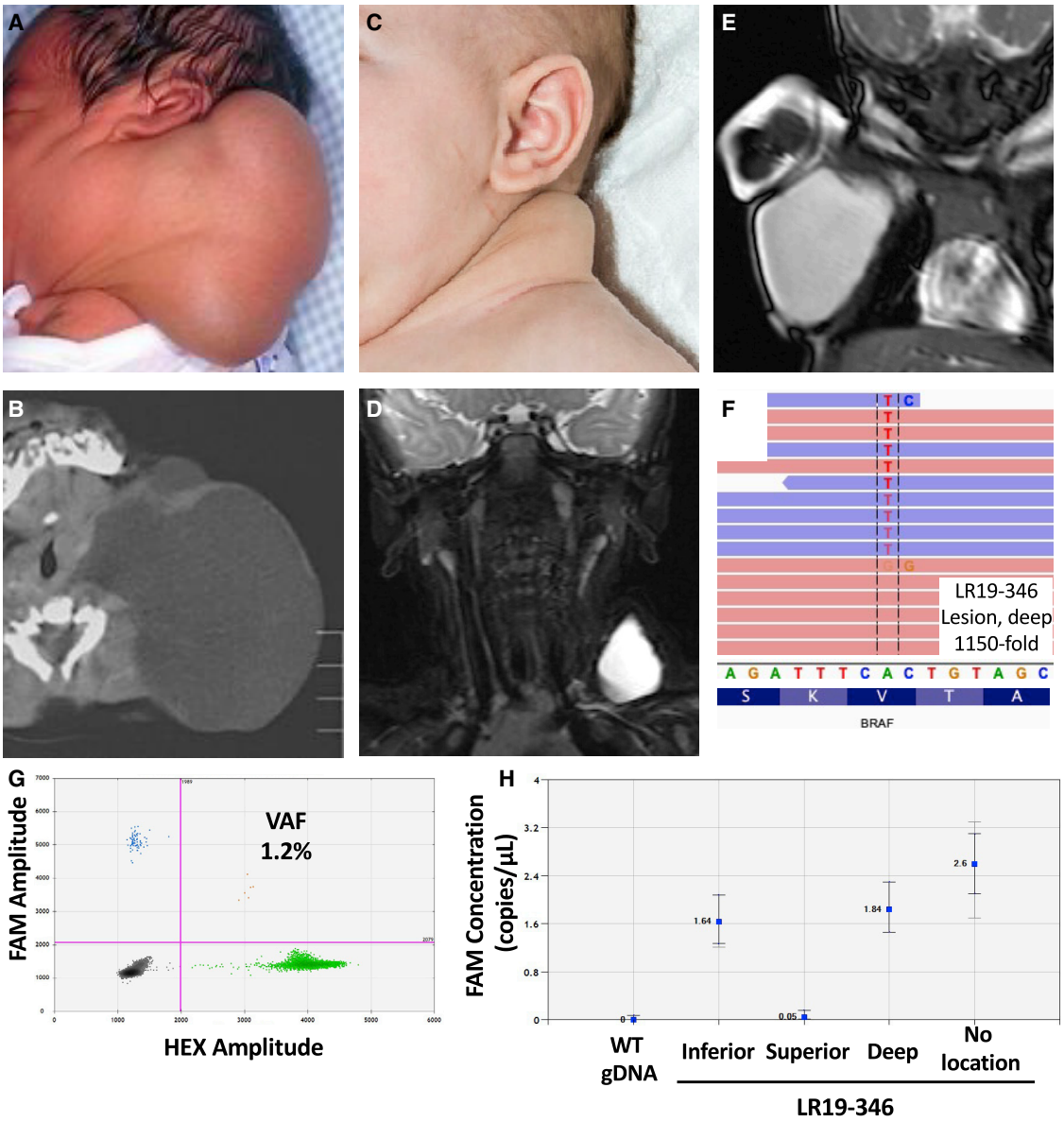

Figure 1. Clinical features of *BRAF*-mutated LM and confirmation of genetic diagnosis

(A–G) Clinical photos of LR17-322 (A) and LR19-346 (C), showing posterior neck LMs. Corresponding computed tomography (CT) (LR17–322; B) and MRI (LR19-346, D; LR19-443, E) images demonstrate macrocystic lesions with minimal septations of the posterior lateral neck and axilla. Integrated Genomics Viewer image for LR19-346 demonstrates somatic BRAF p.Val600Glu variant (F), confirmed on droplet digital PCR (G).

(H) Variant concentration image from Quantasoft shows variability in mutation prevalence between samples (H).

Note: (A) and (B) were previously published prior to identification of this individual's genetic variant.[43]

possible to prove it, we suspect this resulted from a sample swap during the original screening. Poor sample quality could also be a factor, as LR16-265 had lower than typical coverage on VANseq (Table 1). These examples highlight difficulties in using tiered screening assays, which increase the likelihood of sample swaps, and also demonstrate consideration for repeat testing when the diagnostic pre-test probability is high.[20] Previous publications from our lab and others have highlighted the utility of repeat testing when the diagnostic pre-test probability is high.[2,21] We are confident that the pathogenic variant has now been identified for both of these individuals.

VANseq identified a pathogenic *BRAF* variant in 3 of the 15 LMs without a detected *PIK3CA* variant (LR17-322, LR19-346, and LR19-443). All three possessed the same variant (GenBank: NM_004333.6:c.1799T>A, resulting in p.Val600Glu), which was confirmed by ddPCR in multiple independent tissues, when available (Table 1; Figures 1F–1H). Three additional LMs without a detected *PIK3CA* variant (LR17-134, LR17-319, and LR18-572) possessed three or more reads supporting the *BRAF* p.Val600Glu substitution but were not confirmed by ddPCR so were not classified as being *BRAF* positive (Table S2). The presence of three or four alternate base calls out of 1,200–1,500 reads

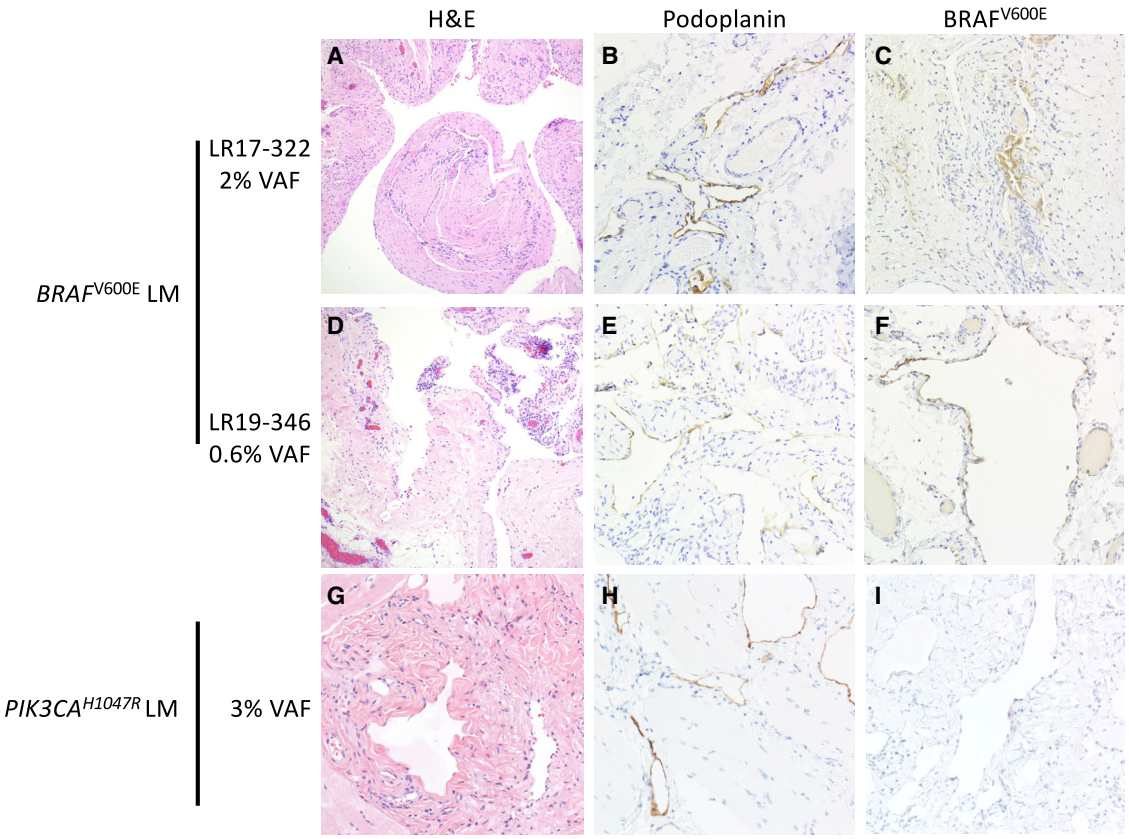

Figure 2. Histology and immunohistochemistry of *PIK3CA* and *BRAF* mutated LMs
LM tissue from two individuals with BRAF p.Val600Glu substitutions (A–F) and one individual with PIK3CA p.His1047Arg substitution. (G–I). H&E stains (A), (D), and (G) show dilated cystic channels with bland, flattened epithelium. (B), (E), and (H) show presence of podoplanin (a.k.a. D2-40) immunoreactivity in endothelial cells. Panels on the right show BRAF p.Val600Glu immunoreactivity (VE1 staining) in endothelial cells in BRAF mutant LM (C and F), but not in PIK3CA mutant LM (I).

is comparable to the inherent error rate of next-generation sequencing (NGS).[22] The discrepancy between the VANseq and ddPCR results for these three samples reflects the lower error rate of ddPCR and highlights the challenges in accurate detection of variants with extremely low allele frequency.

All three individuals with BRAF p.Val600Glu substitutions had macrocystic LMs diagnosed at birth (Figure 1). LR17-322 had a large, macrocystic lesion of the posterior neck, de Serres stage 1, that resolved spontaneously over the first few months of life (Figures 1A and 1B). Surgery was performed at 1 year of age to remove remaining LM and redundant skin. LR19-346's LM was also isolated to the neck, de Serres stage 1, and was resolving with just observation until an upper respiratory infection induced swelling and the decision was made to remove it surgically (Figures 1C and 1D). LR19-443 had a large macrocystic LM of the axilla that was treated with sclerotherapy at 1 month of age (Figure 1E). This individual did not have surgery, but cell free DNA (cfDNA) from aspirated cyst fluid was available for genetic diagnosis. All individuals did well after intervention with no evidence of recurrence and no further procedures or therapy.

Histopathological examination of tissues from two *BRAF* p.Val600Glu containing LMs showed numerous dilated cystic channels with bland, flattened epithelium that was immunopositive for podoplanin, a marker of lymphatic endothelial cells (Figure 2).[23] There were no distinguishing histopathological features between *BRAF* and *PIK3CA* mutant LMs. The extremely low VAFs of the BRAF p.Val600Glu substitutions (0.3%–2%) indicate that most cells within the malformation do not possess the BRAF substitution.[2] We hypothesized that *BRAF* mutant cells would be primarily located within the lymphatic endothelial cells, as has previously been shown in LMs with *PIK3CA* mutations.[24–27] To test this, we used a BRAF p.Val600Glu-specific monoclonal antibody (VE1).[28] BRAF p.Val600Glu immunostaining was present in cyst-lining endothelial cells in LR17-322 and LR19-346, but not in other cells within the lesion (Figure 2). We detected no BRAF p.Val600Glu staining in two other LM samples bearing p.Glu545Lys and p.His1047Arg PIK3CA substitutions (Figure 2; data not shown), demonstrating specificity. These results both confirm the presence of the BRAF substitutions within these lesions and demonstrate their localization to lymphatic endothelial cells.

When these results are combined with our previous reports,[2,29] a more complete picture of allelic and locus heterogeneity within isolated LMs appears (Table 2). *PIK3CA* variants were found in 88% of the 101 individuals in our

Table 2. The genetic spectrum of LM, including *BRAF* p.Val600Glu

	PIK3CA					*BRAF*	
	p.His1047Arg	**p.Glu545Lys**	**p.Glu542Lys**	**Other**	**Total**	**p.Val600Glu**	**NEG[a]**
Zenner et al.[2]	22	18	18	6	64	–	–
Zenner et al.[29]	7	9	5	0	21	–	–
Current study	1	2	0	1	4	3	9
Total, n = 101[b]	30	29	23	7	89 (88.1%)	3 (3.0%)	9 (8.9%)

[a]All negative samples for the first two studies were included in this study if adequate sample was available for VANseq testing.
[b]Total includes only individuals with detected mutations or sufficient DNA to undergo VANseq testing.

cohort, 92% of which occurred at one of the three *PIK3CA* hotspots. *BRAF* p.Val600Glu variants were found in 3% of individuals with isolated LMs—a small proportion but a clinically important finding, as responses to targeted drug therapies may differ. For example, some BRAF inhibitors produce paradoxical activation of the MAPK pathway and corresponding cellular proliferation in tumors possessing oncogenic mutations in RAS or upstream receptors.[30,31] The application of VANseq to our cohort of 101 individuals with isolated LMs brought our overall diagnostic rate from ~80% to over 90%, and currently, only 9/101 individuals with adequate DNA now remain without a genetic diagnosis.[2]

BRAF is one of the most frequently mutated genes in cancer with a predilection for melanoma, thyroid cancer, colon cancer, and non-small cell lung cancer. p.Val600Glu is the most common oncogenic BRAF substitution, accounting for >90% of *BRAF* mutations.[32] Non-mosaic constitutional missense and in-frame deletions in *BRAF* have been reported in RASopathies (e.g., Cardiofaciocutaneous syndrome, Noonan syndrome, and Noonan syndrome with multiple lentigines),[33] but the p.Val600Glu substitution has never been reported in these diseases. This is likely due to the fact that the BRAF p.Val600Glu substitution is not compatible with embryonic survival except in the mosaic state (i.e., the Happle hypothesis).[34] This conclusion is supported by the embryonic lethality seen in constitutional expression of *BRAF* p.Val600Glu in mouse embryos.[35] Somatic *BRAF* p.Val600Glu variants have previously been reported to cause AVMs, though activating mutations in *KRAS* and *MAP2K1* are more common causes.[3,36,37] The precise mechanisms by which somatic BRAF p.Val600Glu substitutions cause LMs in some cases and AVMs in others likely has to do with the timing and location of the post-zygotic mutation. Additional studies are needed to examine this further. Although activating mutations in oncogenes raise concern for an increased risk of cancer, *PIK3CA*-related overgrowth syndromes have a low risk[18] and *BRAF* p.Val600Glu variants are detected in >80% of benign melanocytic nevi, indicating that the single mutation is insufficient to produce melanoma.[38]

All three individuals with *BRAF* p.Val600Glu substitutions in our study had similar clinical phenotypes—large, macrocystic lesions of the neck or body that resolved spontaneously or were treated very early in life. Under the surgical staging system for LMs (de Serres staging), these three individuals would be classified as having stage 1 lesions (unilateral and below the hyoid).[39] Stage 1 lesions make up only ~31% of total LMs in recent studies,[2,39,40] suggesting that the LMs with *BRAF* mutations may represent a milder phenotype than LMs with *PIK3CA* mutations. Although our cohort of LMs with *BRAF* mutations (n = 3) is too small for genotype-phenotype correlations, we speculate that there may be enrichment for *BRAF* mutations in individuals with milder, non-surgical LMs, as genetic diagnosis in most LMs to date has required surgically resected tissue. Additional studies of more LMs with *BRAF* variants, perhaps using non-invasive diagnostic methods, such as cyst-fluid-based cfDNA,[29] will be needed to provide a more balanced view of the genetic spectrum among LMs. The presence of pathogenic *BRAF* variants within the cyst fluid of macrocystic LMs is consistent with our previous study identifying pathogenic *PIK3CA* variants within this compartment.[29] Further studies are needed to assess the relative yield of cyst fluid versus tissue as a diagnostic analyte.

Endothelial cells play a key role in the pathogenesis of vascular malformations, and isolation of endothelial cells from these lesions enriches the detection of somatic variants.[24–27] Prior work in AVMs has shown *KRAS*-mutation-specific staining of endothelial cells,[41] but this has not previously been possible for LMs, as there is no *PIK3CA*-mutant-specific antibody. The presence of $BRAF^{V600E}$ staining in lymphatic endothelial cells within the lesions supports the hypothesis that cell-non-autonomous effects, such as signaling to or recruitment of wild-type cells to the lesion, contribute to the formation of LMs. Cell-non-autonomous effects have been previously suggested to cause cartilage overgrowth in AVMs, but additional studies will be needed to examine this further.[42]

In conclusion, we demonstrate that a somatic activating pathogenic *BRAF* variant (c.1799T>A, [p.Val600Glu]) is present in 3% of our cohort of individuals with isolated lymphatic malformations. Screening isolated LMs for the three PIK3CA hotspots is an efficient and cost-effective approach but will potentially miss clinically important non-hotspot *PIK3CA* and *BRAF* variation. Our use of

VANseq, a high-depth, full-gene sequencing panel, increased the positivity rate for our cohort of LM from ~80% to >90%. In addition, our results suggest the need for studies to examine the efficacy of BRAF inhibition in the treatment of lymphatic malformations.

Data and code availability

The published article includes all data generated or analyzed during this study.

Supplemental information

Supplemental information can be found online at https://doi.org/10.1016/j.xhgg.2022.100101.

Acknowledgments

We thank the participants and their families. This study was funded by the US National Institutes of Health under National Heart, Lung, and Blood Institute (NHLBI) grants F32HL147398(to K.Z.) and R01 HL130996(to J.T.B.), as well as a Burroughs Wellcome Career Award for Medical Scientists 1014700 (to J.T.B.) and a Seattle Children's Hospital Guild Association Funding Focus Award (to J.A.P.). We also acknowledge the Seattle Children's Vascular Anomalies Program and especially the interventional radiology team for their support in sample collection, as well as Dr. Raj Kapur for his assistance with pathology. The content of this work is solely the responsibility of the authors and does not necessarily represent the official views of the funding sources.

Declaration of interests

R.A.B. is a co-founder of EigenHealth, Inc; a consultant to SpiWay, LLC; and holds a financial interest of ownership equity with Wavely Diagnostics, Inc. The remaining authors declare no competing interests.

Received: November 8, 2021
Accepted: March 10, 2022
Published: April 14, 2022

Web resources

Catalogue of Somatic Mutations in Cancer, https://cancer.sanger.ac.uk/cosmic.

Seattle Children's Hospital Lab Test Catalogue, Vascular Anomaly Sequencing Panel (VANSeq) https://seattlechildrenslab.testcatalog.org/show/LAB1920-1.

References

1. Luks, V.L., Kamitaki, N., Vivero, M.P., Uller, W., Rab, R., Bovee, J.V., Rialon, K.L., Guevara, C.J., Alomari, A.I., Greene, A.K., et al. (2015). Lymphatic and other vascular malformative/overgrowth disorders are caused by somatic mutations in PIK3CA. J. Pediatr. *166*, 1048–1054, e1041-1045.
2. Zenner, K., Cheng, C.V., Jensen, D.M., Timms, A.E., Shivaram, G., Bly, R., et al. (2019). Genotype correlates with clinical severity in PIK3CA-associated lymphatic malformations. JCI Insight. *4*, e129884.
3. Al-Olabi, L., Polubothu, S., Dowsett, K., Andrews, K.A., Stadnik, P., Joseph, A.P., Knox, R., Pittman, A., Clark, G., Baird, W., et al. (2018). Mosaic RAS/MAPK variants cause sporadic vascular malformations which respond to targeted therapy. J. Clin. Invest. *128*, 1496–1508.
4. Padia, R., Bly, R., Bull, C., Geddis, A.E., and Perkins, J. (2018). Medical management of vascular anomalies. Curr. Treat Options Pediatr. *4*, 221–236.
5. Adams, D.M., Trenor, C.C., 3rd, Hammill, A.M., Vinks, A.A., Patel, M.N., Chaudry, G., Wentzel, M.S., Mobberley-Schuman, P.S., Campbell, L.M., Brookbank, C., et al. (2016). Efficacy and safety of sirolimus in the treatment of complicated vascular anomalies. Pediatrics *137*, e20153257.
6. Edwards, E.A., Phelps, A.S., Cooke, D., Frieden, I.J., Zapala, M.A., Fullerton, H.J., et al. (2020). Monitoring arteriovenous malformation response to genotype-targeted therapy. Pediatrics *146*, e20193206.
7. Hammer, J., Seront, E., Duez, S., Dupont, S., Van Damme, A., Schmitz, S., Hoyoux, C., Chopinet, C., Clapuyt, P., Hammer, F., et al. (2018). Sirolimus is efficacious in treatment for extensive and/or complex slow-flow vascular malformations: a monocentric prospective phase II study. Orphanet J. Rare Dis. *13*, 191.
8. Lekwuttikarn, R., Lim, Y.H., Admani, S., Choate, K.A., and Teng, J.M.C. (2019). Genotype-guided medical treatment of an arteriovenous malformation in a child. JAMA Dermatol. *155*, 256–257.
9. Parker, V.E.R., Keppler-Noreuil, K.M., Faivre, L., Luu, M., Oden, N.L., De Silva, L., Sapp, J.C., Andrews, K., Bardou, M., Chen, K.Y., et al. (2019). Safety and efficacy of low-dose sirolimus in the PIK3CA-related overgrowth spectrum. Genet. Med. *21*, 1189–1198.
10. Triana, P., Dore, M., Cerezo, V.N., Cervantes, M., Sanchez, A.V., Ferrero, M.M., Gonzalez, M.D., and Lopez-Gutierrez, J.C. (2017). Sirolimus in the treatment of vascular anomalies. Eur. J. Pediatr. Surg. *27*, 86–90.
11. Venot, Q., Blanc, T., Rabia, S.H., Berteloot, L., Ladraa, S., Duong, J.P., Blanc, E., Johnson, S.C., Hoguin, C., Boccara, O., et al. (2018). Targeted therapy in patients with PIK3CA-related overgrowth syndrome. Nature *558*, 540–546.
12. Brouillard, P., Schlogel, M.J., Homayun Sepehr, N., Helaers, R., Queisser, A., Fastre, E., Boutry, S., Schmitz, S., Clapuyt, P., Hammer, F., et al. (2021). Non-hotspot PIK3CA mutations are more frequent in CLOVES than in common or combined lymphatic malformations. Orphanet J. Rare Dis. *16*, 267.
13. Fruman, D.A., Chiu, H., Hopkins, B.D., Bagrodia, S., Cantley, L.C., and Abraham, R.T. (2017). The PI3K pathway in human disease. Cell *170*, 605–635.
14. Makinen, T., Boon, L.M., Vikkula, M., and Alitalo, K. (2021). Lymphatic malformations: genetics, mechanisms and therapeutic strategies. Circ. Res. *129*, 136–154.
15. Dogruluk, T., Tsang, Y.H., Espitia, M., Chen, F., Chen, T., Chong, Z., Appadurai, V., Dogruluk, A., Eterovic, A.K., Bonnen, P.E., et al. (2015). Identification of variant-specific functions of PIK3CA by rapid phenotyping of rare mutations. Cancer Res. *75*, 5341–5354.
16. Gymnopoulos, M., Elsliger, M.A., and Vogt, P.K. (2007). Rare cancer-specific mutations in PIK3CA show gain of function. Proc. Natl. Acad. Sci. U S A *104*, 5569–5574.
17. Lek, M., Karczewski, K.J., Minikel, E.V., Samocha, K.E., Banks, E., Fennell, T., O'Donnell-Luria, A.H., Ware, J.S., Hill, A.J.,

Cummings, B.B., et al. (2016). Analysis of protein-coding genetic variation in 60,706 humans. Nature *536*, 285–291.
18. Gripp, K.W., Baker, L., Kandula, V., Conard, K., Scavina, M., Napoli, J.A., Griffin, G.C., Thacker, M., Knox, R.G., Clark, G.R., et al. (2016). Nephroblastomatosis or Wilms tumor in a fourth patient with a somatic PIK3CA mutation. Am. J. Med. Genet. A. *170*, 2559–2569.
19. Richards, S., Aziz, N., Bale, S., Bick, D., Das, S., Gastier-Foster, J., Grody, W.W., Hegde, M., Lyon, E., Spector, E., et al. (2015). Standards and guidelines for the interpretation of sequence variants: a joint consensus recommendation of the American college of medical genetics and genomics and the association for molecular pathology. Genet. Med. *17*, 405–424.
20. Akobeng, A.K. (2007). Understanding diagnostic tests 2: likelihood ratios, pre- and post-test probabilities and their use in clinical practice. Acta Paediatr. *96*, 487–491.
21. Djemie, T., Weckhuysen, S., von Spiczak, S., Carvill, G.L., Jaehn, J., Anttonen, A.K., Brilstra, E., Caglayan, H.S., de Kovel, C.G., Depienne, C., et al. (2016). Pitfalls in genetic testing: the story of missed SCN1A mutations. Mol. Genet. Genomic Med. *4*, 457–464.
22. Stoler, N., and Nekrutenko, A. (2021). Sequencing error profiles of Illumina sequencing instruments. NAR Genom Bioinform. *3*, lqab019.
23. Fukunaga, M. (2005). Expression of D2-40 in lymphatic endothelium of normal tissues and in vascular tumours. Histopathology *46*, 396–402.
24. Blesinger, H., Kaulfus, S., Aung, T., Schwoch, S., Prantl, L., Rosler, J., Wilting, J., and Becker, J. (2018). PIK3CA mutations are specifically localized to lymphatic endothelial cells of lymphatic malformations. PLoS One *13*, e0200343.
25. Boscolo, E., Coma, S., Luks, V.L., Greene, A.K., Klagsbrun, M., Warman, M.L., and Bischoff, J. (2015). AKT hyper-phosphorylation associated with PI3K mutations in lymphatic endothelial cells from a patient with lymphatic malformation. Angiogenesis *18*, 151–162.
26. Glaser, K., Dickie, P., Neilson, D., Osborn, A., and Dickie, B.H. (2018). Linkage of metabolic defects to activated PIK3CA alleles in endothelial cells derived from lymphatic malformation. Lymphat *16*, 43–55.
27. Osborn, A.J., Dickie, P., Neilson, D.E., Glaser, K., Lynch, K.A., Gupta, A., and Dickie, B.H. (2015). Activating PIK3CA alleles and lymphangiogenic phenotype of lymphatic endothelial cells isolated from lymphatic malformations. Hum. Mol. Genet. *24*, 926–938.
28. Ritterhouse, L.L., and Barletta, J.A. (2015). BRAF V600E mutation-specific antibody: a review. Semin. Diagn. Pathol. *32*, 400–408.
29. Zenner, K., Jensen, D.M., Cook, T.T., Dmyterko, V., Bly, R.A., Ganti, S., Mirzaa, G.M., Dobyns, W.B., Perkins, J.A., and Bennett, J.T. (2021). Cell-free DNA as a diagnostic analyte for molecular diagnosis of vascular malformations. Genet. Med. *23*, 123–130.
30. Cichowski, K., and Janne, P.A. (2010). Drug discovery: inhibitors that activate. Nature *464*, 358–359.
31. Hatzivassiliou, G., Song, K., Yen, I., Brandhuber, B.J., Anderson, D.J., Alvarado, R., Ludlam, M.J., Stokoe, D., Gloor, S.L., Vigers, G., et al. (2010). RAF inhibitors prime wild-type RAF to activate the MAPK pathway and enhance growth. Nature *464*, 431–435.
32. Forbes, S.A., Beare, D., Boutselakis, H., Bamford, S., Bindal, N., Tate, J., Cole, C.G., Ward, S., Dawson, E., Ponting, L., et al. (2017). COSMIC: somatic cancer genetics at high-resolution. Nucleic Acids Res. *45*, D777–D783.
33. Sarkozy, A., Carta, C., Moretti, S., Zampino, G., Digilio, M.C., Pantaleoni, F., Scioletti, A.P., Esposito, G., Cordeddu, V., Lepri, F., et al. (2009). Germline BRAF mutations in Noonan, LEOPARD, and cardiofaciocutaneous syndromes: molecular diversity and associated phenotypic spectrum. Hum. Mutat. *30*, 695–702.
34. Happle, R. (1987). Lethal genes surviving by mosaicism: a possible explanation for sporadic birth defects involving the skin. J. Am. Acad. Dermatol. *16*, 899–906.
35. Mercer, K., Giblett, S., Green, S., Lloyd, D., DaRocha Dias, S., Plumb, M., Marais, R., and Pritchard, C. (2005). Expression of endogenous oncogenic V600EB-raf induces proliferation and developmental defects in mice and transformation of primary fibroblasts. Cancer Res. *65*, 11493–11500.
36. Goss, J.A., Huang, A.Y., Smith, E., Konczyk, D.J., Smits, P.J., Sudduth, C.L., Stapleton, C., Patel, A., Alexandrescu, S., Warman, M.L., et al. (2019). Somatic mutations in intracranial arteriovenous malformations. PLoS One *14*, e0226852.
37. Hong, T., Yan, Y., Li, J., Radovanovic, I., Ma, X., Shao, Y.W., Yu, J., Ma, Y., Zhang, P., Ling, F., et al. (2019). High prevalence of KRAS/BRAF somatic mutations in brain and spinal cord arteriovenous malformations. Brain *142*, 23–34.
38. Pollock, P.M., Harper, U.L., Hansen, K.S., Yudt, L.M., Stark, M., Robbins, C.M., Moses, T.Y., Hostetter, G., Wagner, U., Kakareka, J., et al. (2003). High frequency of BRAF mutations in nevi. Nat. Genet. *33*, 19–20.
39. de Serres, L.M., Sie, K.C., and Richardson, M.A. (1995). Lymphatic malformations of the head and neck. A proposal for staging. Arch. Otolaryngol. Head Neck Surg. *121*, 577–582.
40. Bonilla-Velez, J., Whitlock, K.B., Ganti, S., Zenner, K., Cheng, C.V., Jensen, D.M., Pham, M.M., Mitchell, R.M., Dobyns, W., Bly, R.A., et al. (2021). Acetylsalicylic acid suppression of the PI3K pathway as a novel medical therapy for head and neck lymphatic malformations. Int. J. Pediatr. Otorhinolaryngol. *151*, 110869.
41. Oka, M., Kushamae, M., Aoki, T., Yamaguchi, T., Kitazato, K., Abekura, Y., Kawamata, T., Mizutani, T., Miyamoto, S., and Takagi, Y. (2019). KRAS G12D or G12V mutation in human brain arteriovenous malformations. World Neurosurg. *126*, e1365–e1373.
42. Konczyk, D.J., Goss, J.A., Smits, P.J., Sudduth, C.L., Al-Ibraheemi, A., and Greene, A.K. (2020). Arteriovenous malformation MAP2K1 mutation causes local cartilage overgrowth by a cell-non autonomous mechanism. Sci. Rep. *10*, 4428.
43. Perkins, J.A., Maniglia, C., Magit, A., Sidhu, M., Manning, S.C., and Chen, E.Y. (2008). Clinical and radiographic findings in children with spontaneous lymphatic malformation regression. Otolaryngol. Head Neck Surg. *138*, 772–777.

HGGA, Volume *3*

Supplemental information

Somatic activating *BRAF* variants cause isolated lymphatic malformations

Kaitlyn Zenner, Dana M. Jensen, Victoria Dmyterko, Giridhar M. Shivaram, Candace T. Myers, Cate R. Paschal, Erin R. Rudzinski, Minh-Hang M. Pham, V. Chi Cheng, Scott C. Manning, Randall A. Bly, Sheila Ganti, Jonathan A. Perkins, and James T. Bennett

Supplemental Information

TABLE OF CONTENTS **Page**

Table S1: Gene Content of VANSeq

ACVRL1	*EPHB4*	*GNA14*	*MAP3K3*	*SMAD4*
ARAF	*FAT4*	*GNAQ*	*MET*	*SOX18*
BRAF	*FGFR1*	*HGF*	*NRAS*	*TEK*
CCBE1	*FLT4*	*HRAS*	*PCDC10*	*VEGFC*
CCM2	*FOXC2*	*IDH1*	*PDGFRB*	
CELSR1	*GATA2*	*IDH2*	*PIEZO1*	
CTNNB1	*GDF2*	*KIF11*	*PIK3CA*	
DCHS1	*GJC2*	*KRAS*	*PTEN*	
ELMO2	*GLMN*	*KRIT1*	*PTPN14*	
ENG	*GNA11*	*MAP2K1*	*RASA1*	

Table S2: *BRAF* p.V600E variants on VANseq and ddPCR

	VANseq			ddPCR			
Subject	Reference count	Variant count	VAF (%)	Reference count	Variant count	VAF[a] (%)	Variant detected?
LR17-322	1618	34	2.1	10,555	165	1.7	Yes
LR19-346	1143	7	0.6	5872	69	1.2	Yes
LR19-443	1458	4	0.3	9661	10	0.1	Yes
LR17-134	1507	4[b]	0.3	7756	0	NEG	No
LR17-319	1256	4[b]	0.3	10,850	0	NEG	No
LR18-572	1420	3[b]	0.2	10,558	0	NEG	No

Abbreviations: ddPCR – droplet digital polymerase chain reaction, NEG – no variant detected, VAF – variant allele fraction

[a]ddPCR VAF calculated using droplet concentrations and only reported for samples in which sample variant concentration was statistically different from wild-type control variant concentration based on 95% total error confidence intervals.

[b]The presence of 3-4 alternate base calls out of 1200-1500 reads is comparable to the inherent error rate of NGS.[1] The discrepancy between VANseq and ddPCR is explained by the much lower error rate of ddPCR.

Supplemental Methods

Participants and sample collection

This study was approved by the Institutional Review Board at Seattle Children's Hospital. Written, informed consent was obtained for each individual in this study prior to sample and data collection. All individuals presented are de-identified. We included all individuals with isolated LMs treated at Seattle Children's Hospital between 2000 and 2020 who had LM tissue available for analysis. Individuals with accompanying overgrowth syndromes such as fibro-adipose vascular anomaly (FAVA), Klippel-Trenaunay syndrome (KTS), and congenital lipomatosis, overgrowth, vascular malformations, epidermal nevi, and skeletal/spinal anomalies (CLOVES) were excluded. LM tissue was prospectively collected at clinically indicated surgical procedures, flash frozen, and stored in a biorepository at -80 degrees Celsius. DNA from lesions was isolated with PureLink Genomic DNA Mini Kit (Invitrogen, Carlsbad, CA). Blood and cyst fluid were collected in either EDTA tubes or Cell-Free DNA BCT® tubes ("Streck tubes", Streck Omaha, NE). Cyst fluid was collected during surgery or sclerotherapy, or in clinic with ultrasound guidance. cfDNA was isolated as previously described.[2] Many of the individuals included in this study were previously reported and are indicated as such in corresponding figures and tables. In cases where samples were screened by more than one method (e.g ddPCR and high depth NGS), the same aliquot of DNA was utilized.

ddPCR screening

Bio-Rad-designed droplet digital PCR (ddPCR) assays were used to screen the three most common *PIK3CA* mutations in LM: p.Glu542Lys, p.Glu545Lys, and p.His1047Arg (Bio-Rad, Hercules, CA) as previously described.[3] The less common *PIK3CA* mutation p.His1047**Leu** was also included, simply because it overlaps the p.His1047Arg containing ddPCR amplicon. A subset of samples were screened for these four mutations using a *PIK3CA* multiplex ddPCR as previously reported.[2] Following identification of variants by VANseq, ddPCR assays for *PIK3CA* p.Asn345Lys and *BRAF* p.Val600Glu (Bio-Rad) were used to confirm variants and screen additional samples for variant positive individuals. All PCR reactions were set up in a UV-treated hood with positive air-flow, and reactions were carried out in three or more independent wells to guard against contamination artifacts. Samples were positive if the variant fluorescence was significantly different from the fluorescence of the WT control using 95% confidence intervals for total error. The total error is displayed by the QuantaSoft software and defined as the greater of either the technical error (Poisson error) or the empirical error (standard error of the mean). Variant allele fractions (VAFs) were calculated as the concentration of variant droplets out of the total concentration of droplets containing at least one copy of variant or WT DNA.

Ultra-deep full gene sequencing: VANseq

Target enrichment of 44 genes (**Table S1**) was performed using IDT xGen Predesigned Gene Capture Pools and custom spike-in probes. Target region includes coding exons and a minimum of 10 bp of flanking intron boundaries of the genes tested. Libraries were generated with the IDT xGen Hybridization and Wash Kit following manufacturer's instructions. Libraries were sequenced to an average depth of coverage of 1000x on a Illumina NextSeq 500 with 2x151 bp reads. Reads were aligned with Novoalign Version 2.08.02. Variants were called using samtools (mpileup) Version 0.1.19, Freebayes Version 0.9.21, GATK: Version 1.2, and Pindel: Version 0.2.4d.

Immunohistochemistry

Formalin fixed-paraffin embedded tissue from individuals with *PIK3CA* p.Glu545Lys and *BRAF* p.Val600Glu variants was identified in the pathology archive. Unstained slides were cut at 4 um for immunohistochemistry using the Ventana Ultra platform with the following antibodies: mouse anti-$BRAF^{V600E}$ (1:100; catalog no. ab228461; AbCam), and mouse anti-PDPN (1:10; catalog no 322M-16; Cell Marque).

Supplemental References

1. Stoler, N., and Nekrutenko, A. (2021). Sequencing error profiles of Illumina sequencing instruments. NAR Genom Bioinform 3, lqab019.
2. Zenner, K., Jensen, D.M., Cook, T.T., Dmyterko, V., Bly, R.A., Ganti, S., Mirzaa, G.M., Dobyns, W.B., Perkins, J.A., and Bennett, J.T. (2021). Cell-free DNA as a diagnostic analyte for molecular diagnosis of vascular malformations. Genet Med 23, 123-130.
3. Zenner, K., Cheng, C.V., Jensen, D.M., Timms, A.E., Shivaram, G., Bly, R., Ganti, S., Whitlock, K.B., Dobyns, W.B., Perkins, J., et al. (2019). Genotype correlates with clinical severity in PIK3CA-associated lymphatic malformations. JCI Insight.